Supporting Information

for

Aptamer-based colorimetric detection of the DNA damage marker 8-oxo-dG using cysteamine-stabilized gold nanoparticles

Chadamas Sakonsinsiri[a,b,*], Theerapong Puangmali[c], Kaniknun Srijiwangsa[a], Sireemas Koowattanasuchat[a], Raynoo Thanan[a,b], Apiwat Chompoosor[d], Sirinan Kulchart[e] and Paiboon Sithithaworn[f]

[a] *Department of Biochemistry, Faculty of Medicine, Khon Kaen University, Khon Kaen 40002, Thailand;*

[b] *Cholangiocarcinoma Research Institute, Khon Kaen University, Khon Kaen, Thailand 40002;*

[c] *Department of Physics, Faculty of Science, Khon Kaen University, Khon Kaen 40002, Thailand;*

[d] *Department of Chemistry, Faculty of Science, Ramkhamhaeng University, Bangkok 10240, Thailand;*

[e] *Department of Chemistry, Faculty of Science, Khon Kaen University, Khon Kaen 40002, Thailand;*

[f] *Department of Parasitology, Faculty of Medicine, Khon Kaen University, Khon Kaen 40002, Thailand*

* *Corresponding Author. E-mail: schadamas@kku.ac.th*

Synthesis of cysteamine-stabilized AuNPs (Cyst-AuNPs)

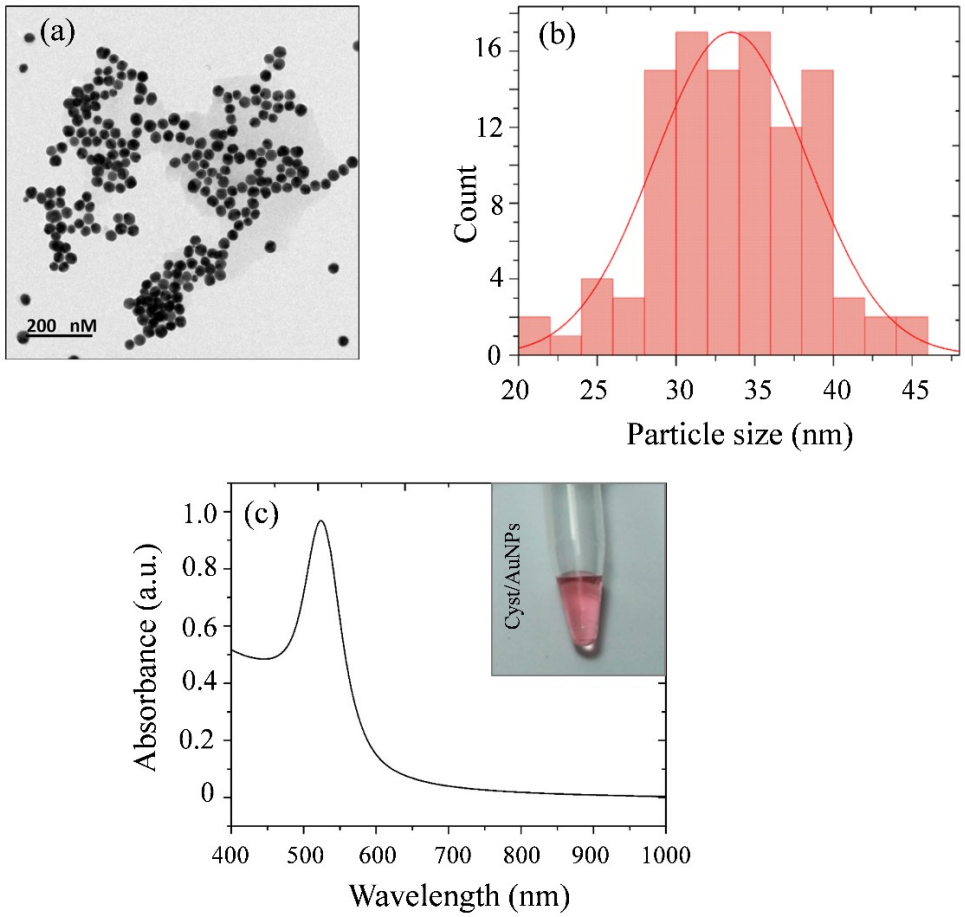

Fig. S1. (a) TEM image of Cyst-AuNPs. (b) Size distribution of Cyst-AuNPs. (c) Absorption spectrum and observation (Inset) of Cyst-AuNPs.

Optimization of the sensing parameters by fixing 8-oxo-dG concentration at 12 nM

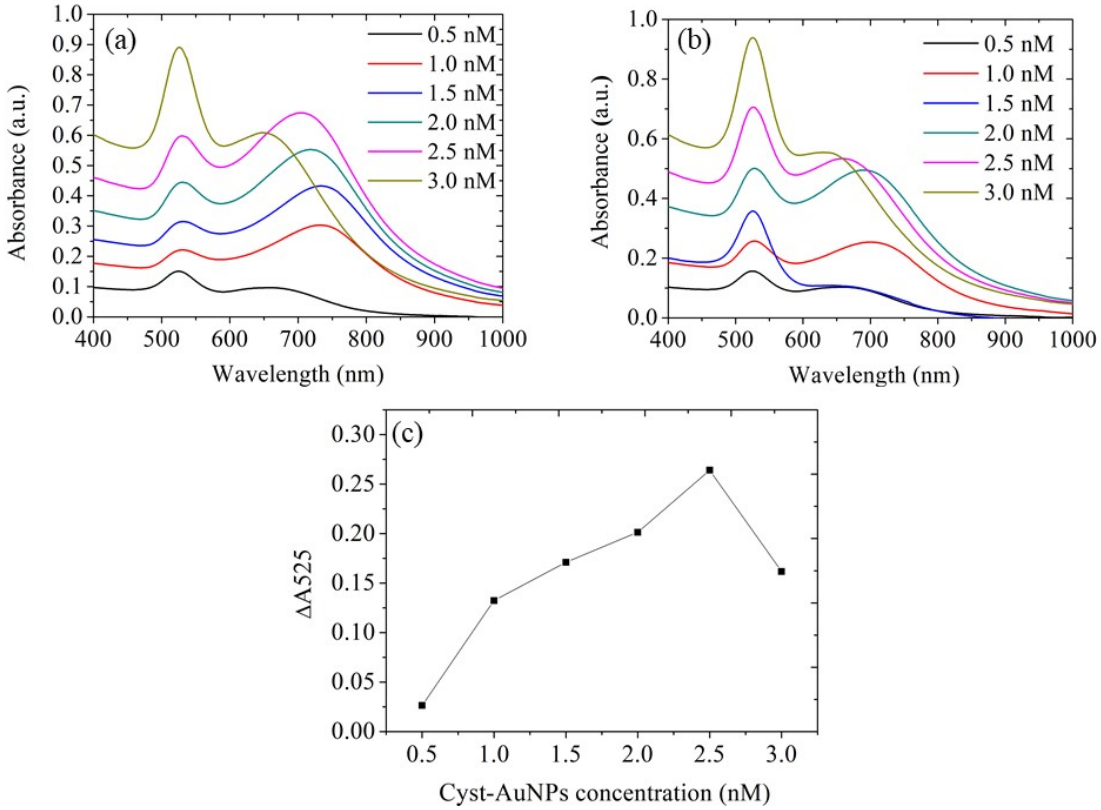

Fig. S2. Effects of Cyst-AuNPs concentrations on the performance of 8-oxo-dG colorimetric detection system: (a) UV-Vis absorption spectra of the Cyst-AuNPs + Aptamer; (b) UV-Vis absorption spectra of the Cyst-AuNPs + Aptamer + 8-oxo-dG; (c) the difference in absorbance at 525 nm (ΔA_{525}). Experimental conditions: Aptamer, 5 nM; 8-oxo-dG, 12 nM; Phosphate buffer, 1 mM, pH 7.0.

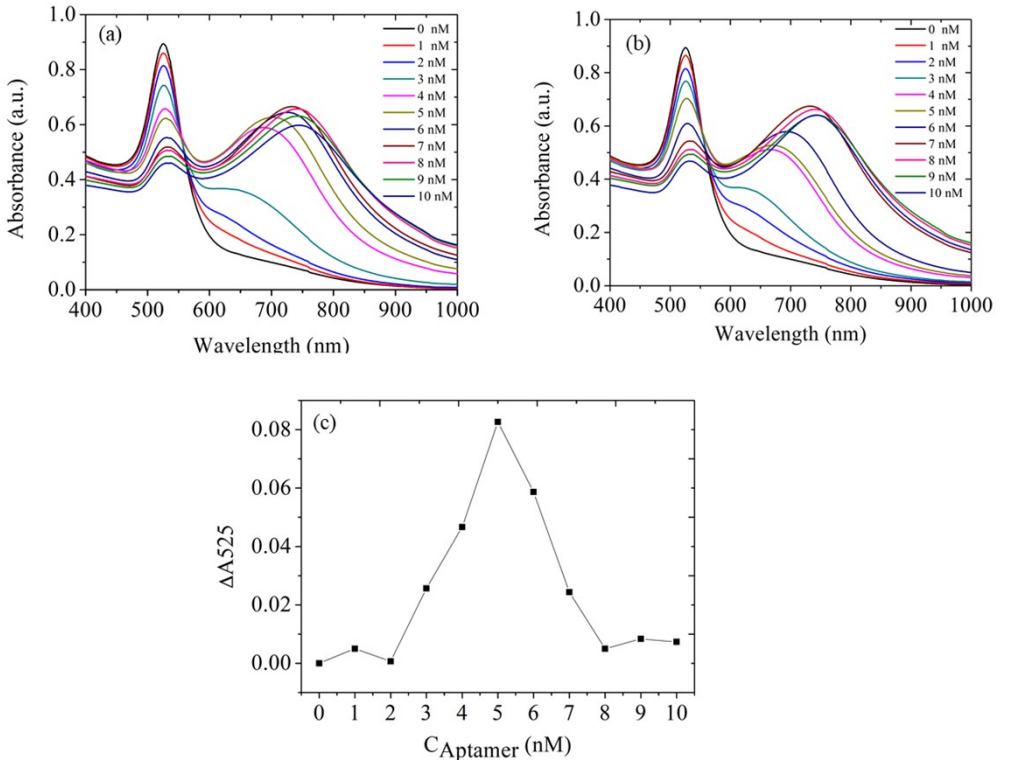

Fig. S3. Effects of aptamer concentrations on the performance of 8-oxo-dG colorimetric detection system: a) UV-Vis absorption spectra of the Cyst-AuNPs + Aptamer; (b) UV-Vis absorption spectra of the Cyst-AuNPs + Aptamer + 8-oxo-dG; (c) the difference in absorbance at 525 nm (ΔA_{525}). The final concentrations of aptamers were 0, 1, 2, 3, 4, 5, 6, 7, 8, 9 and 10 nM. Experimental conditions: Cyst-AuNPs, 2.5 nM; Phosphate buffer, 1 mM, pH 7.0.; 8-oxo-dG, 12 nM.

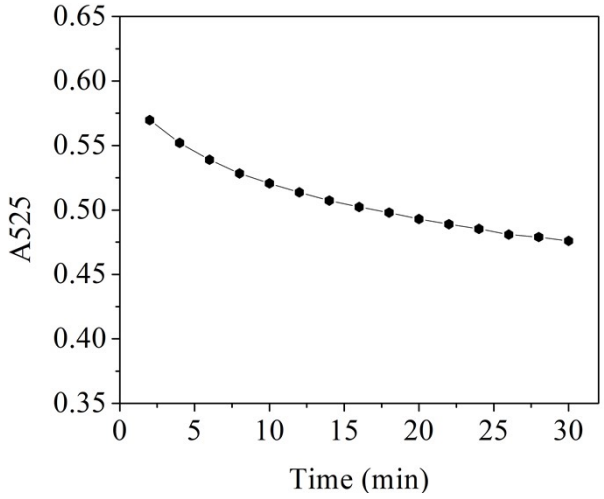

Fig. S4. Optimization of the incubation time of aptamer with Cyst-AuNPs. The concentration of 8-oxo-dG was 12 nM. Experimental conditions: Cyst-AuNPs, 2.5 nM, Aptamer, 5 nM; Phosphate buffer, 1 mM, pH 7.0.

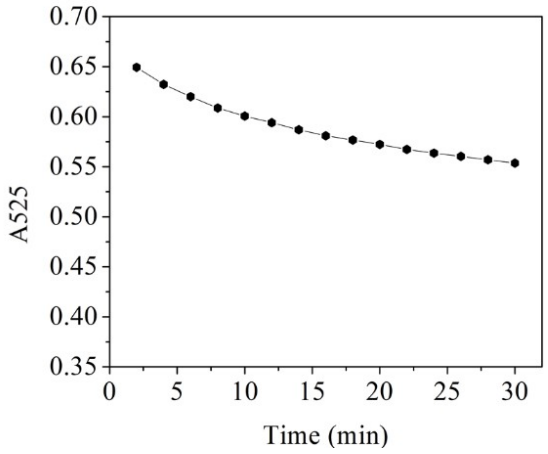

Fig. S5. Optimization of the binding time of aptamer with 8-oxo-dG. Experimental conditions: Cyst-AuNPs, 2.5 nM, Aptamer, 5 nM; 8-oxo-dG, 12 nM; Phosphate buffer, 1 mM, pH 7.0.

Optimization of the sensing parameters by fixing 8-oxo-dG concentration at 50 nM

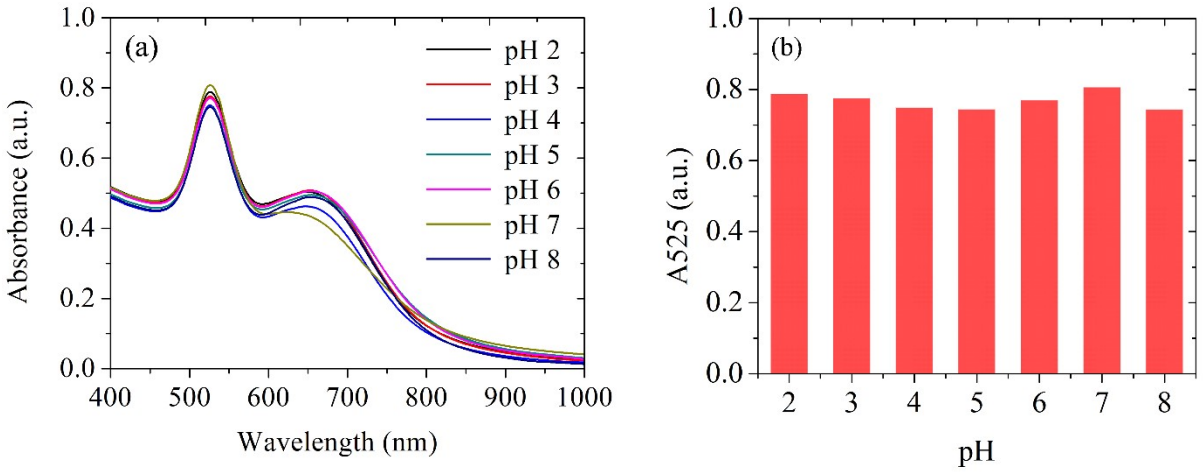

Fig. S6 Effects of pH on the performance of 8-oxo-dG colorimetric detection system: (a) UV-Vis absorption spectra of the 8-oxo-dG colorimetric detection system; (b) The absorbance at 525 nm (A_{525}) at different pH, ranging from 2.0-8.0. Experimental conditions: Cyst-AuNPs, 2.5 nM; Aptamer, 5 nM; 8-oxo-dG, 50 nM.

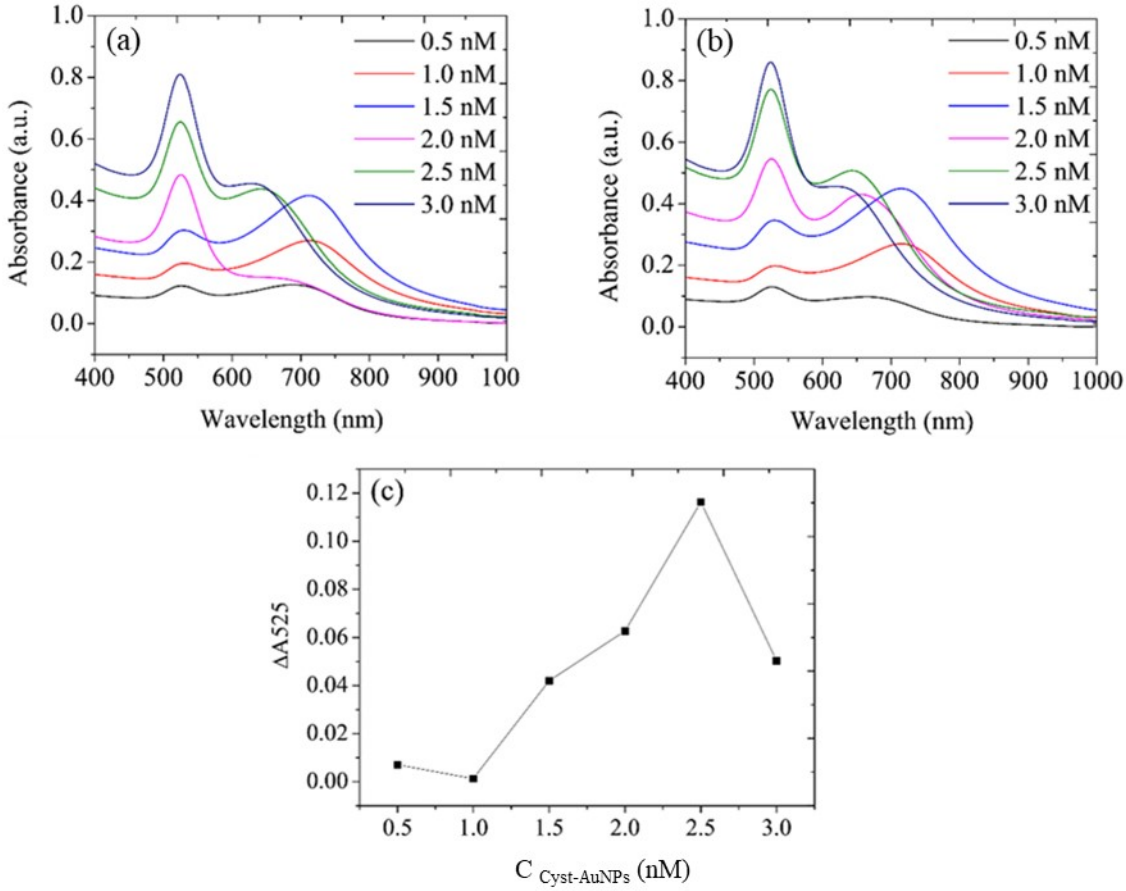

Fig. S7. Effects of Cyst-AuNPs concentrations on the performance of 8-oxo-dG colorimetric detection system: (a) UV-Vis absorption spectra of the Cyst-AuNPs + Aptamer; (b) UV-Vis absorption spectra of the Cyst-AuNPs + Aptamer + 8-oxo-dG; (c) the difference in absorbance at 525 nm (ΔA_{525}). Experimental conditions: Aptamer, 5 nM; 8-oxo-dG, 50 nM; Phosphate buffer, 1 mM, pH 7.0.

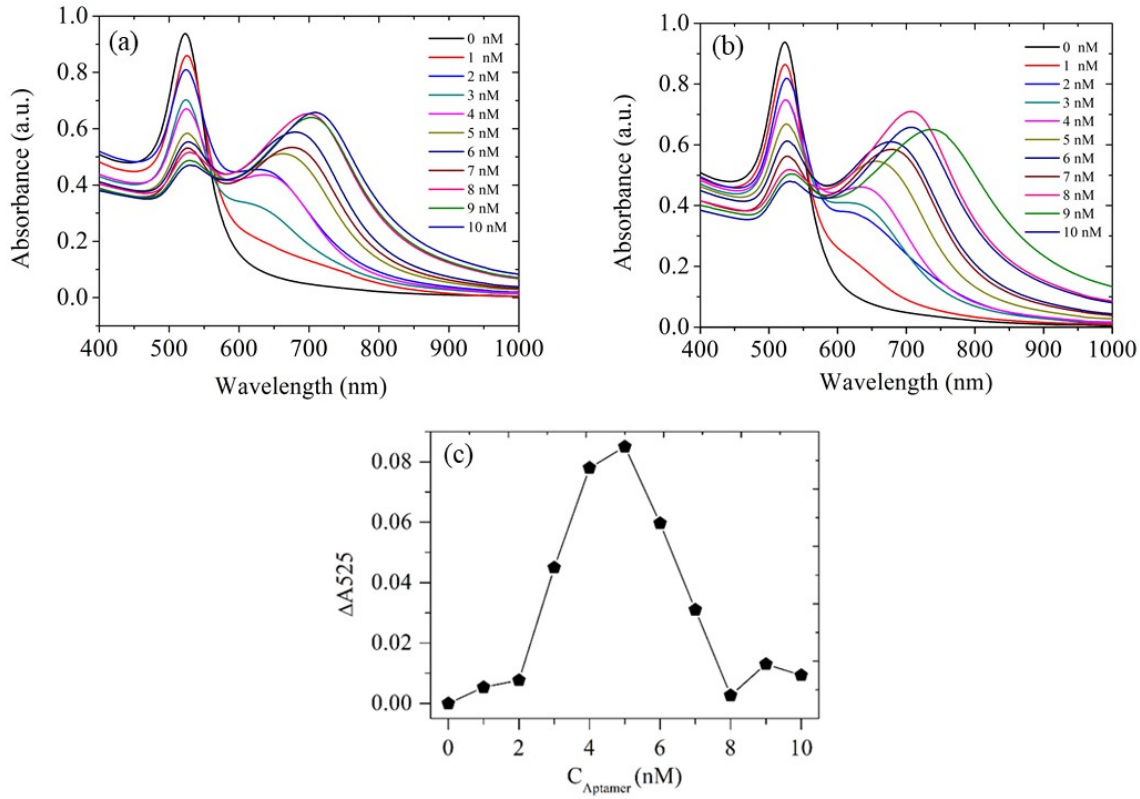

Fig. S8. Effects of aptamer concentrations on the performance of 8-oxo-dG colorimetric detection system: a) UV-Vis absorption spectra of the Cyst-AuNPs + Aptamer; (b) UV-Vis absorption spectra of the Cyst-AuNPs + Aptamer + 8-oxo-dG; (c) the difference in absorbance at 525 nm (ΔA_{525}). The final concentrations of aptamers were 0, 1, 2, 3, 4, 5, 6, 7, 8, 9 and 10 nM. Experimental conditions: Cyst-AuNPs, 2.5 nM; Phosphate buffer, 1 mM, pH 7.0.; 8-oxo-dG, 50 nM.

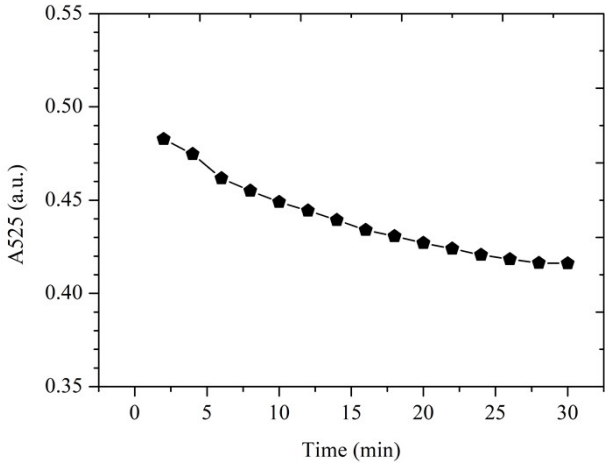

Fig. S9. Optimization of the incubation time of aptamer with Cyst-AuNPs. The concentration of 8-oxo-dG was 50 nM. Experimental conditions: Cyst-AuNPs, 2.5 nM, Aptamer, 5 nM; Phosphate buffer, 1 mM, pH 7.0.

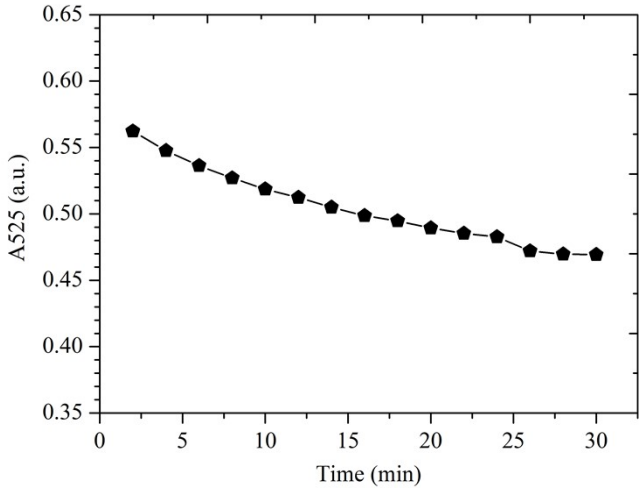

Fig. S10. Optimization of the binding time of aptamer with 8-oxo-dG. Experimental conditions: Cyst-AuNPs, 2.5 nM, Aptamer, 5 nM; 8-oxo-dG, 50 nM; Phosphate buffer, 1 mM, pH 7.0.

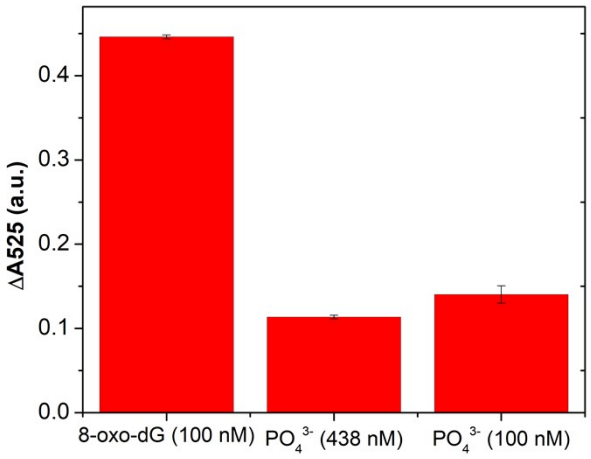

Fig. S11. Specificity of the aptamer-AuNPs-based colorimetric assay for 8-oxo-dG detection comparable to 438 nM and 100 nM PO_4^{3-}. The 8-oxo-dG concentration was 100 nM.

Table S1. Zeta potential and size distribution of the aggregate in the solution.

Sample	Zeta potential (mV)	Size determined by DLS (nm)
Cyst-AuNPs	13.9 ± 0.5	42.9 ± 2.1
Cyst-AuNPs + Aptamer	18.4 ± 1.1	203.2 ± 8.9
Cyst-AuNPs + Aptamer + 8-oxo-dG (10 nM)	16.9 ± 2.9	159.3 ± 10.7
Cyst-AuNPs + Aptamer + 8-oxo-dG (50 nM)	16.4 ± 0.8	131.2 ± 11.8
Cyst-AuNPs + Aptamer + 8-oxo-dG (100 nM)	16.3 ± 0.8	114.6 ± 13.6

Note: All solutions were in phosphate buffer pH (1 mM); 2.5 nM Cyst-AuNPs and 5 nM aptamer were used in all conditions.

Table S2. Intra-day and inter-day precision of the proposed 8-oxo-dG detection method.

Matrix	8-oxo-dG (nM)	Intra-day (n = 3)			Inter-day (n = 15)		
		Mean	S.D.	RSD (%)	Mean	S.D.	RSD (%)
Water	60	66.6	3.8	5.7	67.2	7.1	10.6
	80	86.1	10.5	12.1	86.2	10.5	12.1
Urine	60	67.3	10.0	14.9	71.4	8.9	12.4
	80	83.3	16.4	19.7	86.6	7.2	8.4

S.D., standard deviation. RSD, relative standard deviation calculated as S.D./mean × 100.